578721

Sandia National Laboratories

Operated for the United States Department of Energy
by National Technology and Engineering Solutions
of Sandia, LLC.

Albuquerque, New Mexico 87185-0101
Livermore, California 94551-0969

date: January 30, 2023

to: SNL WIPP[1] Records Center, SNL WIPP Geochemistry
Sandia National Laboratories
4100 National Parks Highway, Building A, Carlsbad, New Mexico 88220, U.S.A.

from: Jay Jang (jjang@sandia.gov)
Sandia National Laboratories
4100 National Parks Highway, Building A, Carlsbad, New Mexico 88220, U.S.A.

subject: The $PbSO_4(s)$ - Na_2SO_4 - NaCl - H_2O Experiment (Revision 0)

I. Drivers

SNL WIPP Geochemistry needs to include thermodynamic quantities[2] for Pb^{+2} - SO_4^{-2} system in the thermodynamic database to represent the speciation of Pb^{+2} in the presence of SO_4^{-2}. The experiment relevant to the Pb^{+2} - SO_4^{-2} system, i.e., the $PbSO_4(s)$ - Na_2SO_4 - NaCl - H_2O experiment, was conducted at ambient laboratory condition, e.g., 24.5±4.3 °C (Arnold and Jang, 2022). The measurements were processed and summarized in Section III.1 of GEOC-21-03 (Jang et al., 2021).

The $PbSO_4(s)$ - Na_2SO_4 - NaCl - H_2O experiment contained Cl^- which forms complexes with Pb^{+2}. The formation of Pb^{+2} - Cl^- complexes would interfere with the interpretation of the affinity between Pb^{+2} and SO_4^{-2} via interaction or complexation. Thus, a prerequisite to the parameterization of the $PbSO_4(s)$ - Na_2SO_4 - NaCl - H_2O experiment was the validation and inclusion of a Pb^{+2} - Cl^- model. If the experiment had been designed without Cl^-, the prerequisite would have been unnecessary.

SNL WIPP Geochemistry installed the thermodynamic parameters for Pb^{+2} - Na^+ - Cl^- - H^+ - H_2O system as summarized in Table IX.2-1 and Table IX.2-2 of GEOC-21-11 (Jang et al., 2021), and is now ready to evaluate and parameterize the results of the $PbSO_4(s)$ - Na_2SO_4 - NaCl - H_2O experiment.

---

[1] SNL WIPP: Sandia National Laboratories at the Waste Isolation Pilot Plant (WIPP). WIPP is located ~26 miles southeast of Carlsbad, New Mexico, U.S.A., built 2,150 feet underground in the Salado Formation, a thick Permian evaporite deposit in the northern Delaware Basin.

[2] Thermodynamic quantities: LogK values of chemical reactions and relevant PIPs.

Information Only
Exceptional Service in the National Interest

SNL WIPP Geochemistry needs to emphasize the importance of experimental validation of the literature-retrieved measurements and thermodynamic quantities, especially for the cases where the thermodynamic quantities in the literature were derived from measurements (i) that were not addressed by their own uncertainty and (ii) of limited range of experimental conditions in the investigation. Parameterizations based on such measurements can be considered highly subjective if the uncertainty of the measurements are not explicitly disclosed. This memo reports an example of such case and the SNL WIPP Geochemistry has been aware of the critical needs of repeating experiments in the same or similar conditions as those in the literature.

II. Chemical System

The Pb^{+2} - SO_4^{-2} system of this memo addresses the solubility of $PbSO_4$(s) (anglesite) in solutions of six incremental concentrations of Na_2SO_4 (0.01, 0.1, 0.5, 1.0, 1.5, 1.8 m) spiked with constant concentration of NaCl at 0.15 m. Excess $PbSO_4$(s) (anglesite) was added to the solutions to prevent the depletion of the solid and to characterize the solid at the end of the experiment. The six system components are Pb^{+2}, Na^+, SO_4^{-2}, Cl^-, H^+, and H_2O.

III. Goals and Hypotheses

The goal of the experiment was to examine how the common ion effect affects the solubility of $PbSO_4$(s), the common ion being SO_4^{-2}, in the presence of constant Cl^- concentration. The hypothesis is that the affinity between Pb^{+2} and SO_4^{-2} ions can be assessed via either ionic interaction or aqueous complexation.

IV. Reactor Preparation

2.0 (or 0.4) grams $PbSO_4$(s) (anglesite, FW[3] = 303.26 g/mol) was added into 100 (or 20) mL solutions representing six different experimental conditions. $PbSO_4$(s) loading was 0.0659 mol/L ≡ 0.066 mol/L as Pb in the six experimental conditions. The solid loading levels and solution composition used in these experiments are given in Table II.1-1 and Table II.1-2 of GEOC-21-03 (Jang et al., 2021). The differences of the solution compositions in the two Tables are less than 2%. The loadings in Table II.1-1 of GEOC-21-03 (Jang et al., 2021) were used in calculating the %Deviations in Table V-3, Table V-4, and Table V-5 of this memo. %Deviation is defined in Equation (1).

$$\%\text{Deviation} = (\text{Average} - \text{Loading})/\text{Loading} \times 100\ (\%) \quad (1)$$

[3] FW means Formular Weight in g/mol.

Information Only

V. Data - Aqueous Chemistry

pHr is the reading in the display of a pH meter when the pH electrode was calibrated using commercial, NIST-scaled pH buffers of low ionic strengths. ΣPb and ΣNa were measured using an ICP-AES. ΣSO4 and ΣCl were measured using an IC.

In the Tables in the following sections, SD means standard deviation, 2SD means twice the standard deviation, %2SD is defined by [2SD/Average × 100 (%)], and count means the number of measurements used to calculate the average and SD.

V.1. pHr

The pHr measurements are summarized in Table III.1-1 and Table III.1-3 of GEOC-21-03 (Jang et al., 2021). They are combined and the statistics are presented in Table V-1.

Table V-1 Statistics of the pHr measurements.

pHr				
Average	SD	2SD	%2SD	Count
2.76	0.12	0.24	9%	20
3.14	0.08	0.17	5%	20
3.47	0.08	0.15	4%	20
3.52	0.10	0.19	6%	19
3.58	0.10	0.20	6%	20
3.58	0.12	0.25	7%	20

V.2. ΣPb

The measurements of ΣPb are summarized in Table III.1-5 and Table III.1-7 of GEOC-21-03 (Jang et al., 2021). They are combined and the statistics are presented in Table V-2.

Table V-2. Statistics of the ΣPb measurements.

ΣPb, M				
Average	SD	2SD	%2SD	Count
6.93E-05	5.78E-06	1.16E-05	17%	21
2.72E-05	6.49E-06	1.30E-05	48%	22
3.37E-05	4.31E-06	8.62E-06	26%	23
4.84E-05	9.64E-06	1.93E-05	40%	24
6.55E-05	1.14E-05	2.29E-05	35%	24
7.71E-05	7.52E-06	1.50E-05	20%	21

Information Only

V.3. ΣSO4

The measurements of ΣSO4 are summarized in Table III.1-9 and Table III.1-11 of GEOC-21-03 (Jang et al., 2021). They are combined and the statistics are presented in Table V-3.

Table V-3. Statistics of the ΣSO4 measurements.

ΣSO4, M					
Average	SD	2SD	%2SD	Count	%Deviation [A]
1.22E-02	2.90E-03	5.80E-03	48%	18	22%
1.05E-01	2.09E-02	4.18E-02	40%	18	5%
4.93E-01	5.68E-02	1.14E-01	23%	20	1%
9.69E-01	7.00E-02	1.40E-01	14%	20	2%
1.40E+00	9.90E-02	1.98E-01	14%	20	1%
1.36E+00	1.19E-01	2.38E-01	18%	20	-18%

[A] Calculated with respect to the loadings in Table II.1-1 of GEOC-21-03 (Jang et al., 2021)

V.4. ΣNa

The measurements of ΣNa are summarized in Table III.1-13 and Table III.1-15 of GEOC-21-03 (Jang et al., 2021). They are combined and the statistics are presented in Table V-4.

Table V-4. Statistics of the ΣNa measurements.

ΣNa, M					
Average	SD	2SD	%2SD	Count	%Deviation [A]
1.64E-01	6.61E-03	1.32E-02	8%	20	-4%
3.32E-01	1.98E-02	3.97E-02	12%	20	-5%
1.05E+00	4.02E-02	8.05E-02	8%	22	-6%
2.04E+00	8.16E-02	1.63E-01	8%	22	0%
2.82E+00	2.03E-01	4.05E-01	14%	22	-4%
2.80E+00	2.84E-01	5.68E-01	20%	22	-19%

[A] Calculated with respect to the loadings in Table II.1-1 of GEOC-21-03 (Jang et al., 2021)

V.5. ΣCl

The measurements of ΣCl are summarized in Table III.1-17 and Table III.1-19 of GEOC-21-03 (Jang et al., 2021). They are combined and the statistics are presented in Table V-5.

Information Only

98 Table V-5. Statistics of the ΣCl measurements.

ΣCl, M					
Average	SD	2SD	%2SD	Count	%Deviation [A]
1.53E-01	4.62E-03	9.23E-03	6%	16	2%
1.49E-01	6.18E-03	1.24E-02	8%	16	0%
1.61E-01	1.89E-02	3.79E-02	24%	18	10%
1.52E-01	1.32E-02	2.65E-02	17%	18	7%
1.50E-01	9.83E-03	1.97E-02	13%	18	8%
1.64E-01	1.13E-02	2.27E-02	14%	18	19%

99 [A] Calculated with respect to the loadings in Table II.1-1 of GEOC-21-03 (Jang et al., 2021)

100

101 ## VI. Data - Solids

102 X-ray diffraction (XRD) scans of the solids are presented in Figure III.1-16 and Figure III.1-17 of
103 GEOC-21-03 (Jang et al., 2021). $PbSO_4$(s) (anglesite) is the only Pb solid observed. At the highest
104 loading of Na_2SO_4 at 1.8 m, Na_2SO_4(s) (thenardite) was observed in Figure III.1-16 of GEOC-21-03.
105 The observation of thenardite is attributed to the precipitation following the evaporation of the Na_2SO_4
106 background solution captured in the pore space of the solid collected. Thenardite was not observed in
107 Figure III.1-17 of GEOC-21-03.

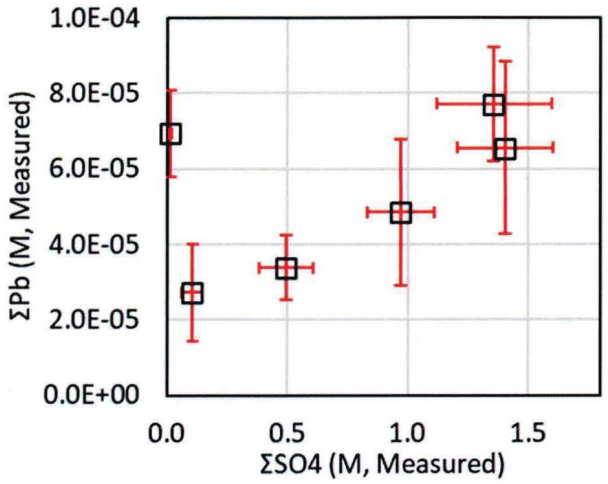
108 ## VII. Observations

109 No systematic changes with time were observed for the system components (Figures and Tables in
110 Section III.1 of GEOC-21-03; Jang et al., 2021). The observed scatter in the data is confined within
111 the maximum %2SD of 48%. The maximum %2SD (i.e., lowest precision of measurements) was
112 observed for ΣPb and ΣSO4 measurements (Table V-2, Table V-3). The total dissolved divalent lead
113 Pb(II) concentration, ΣPb, was less than 10^{-4} M. Thus, the solid was not depleted, and more than 99%
114 Pb(II) added as $PbSO_4$(s) (0.066 mol/L) resides in the solid phase without formation of secondary Pb
115 solids (Figure III.1-16 and Figure III.1-17 of GEOC-21-03). It can be assumed that chemical
116 equilibrium was attained. The effect of CO_2(g) intrusion in the experiment was concluded to be non-
117 identifiable in GEOC-21-03 (Jang et al., 2021).

118 The common ion effect suppressed ΣPb when $0 < \Sigma SO4 < 0.1$ M, and increased ΣPb when $\Sigma SO4 > 0.1$
119 M (Figure VII-1). Through Section VIII, this observation will be attributed to either ionic interaction
120 or complexation.

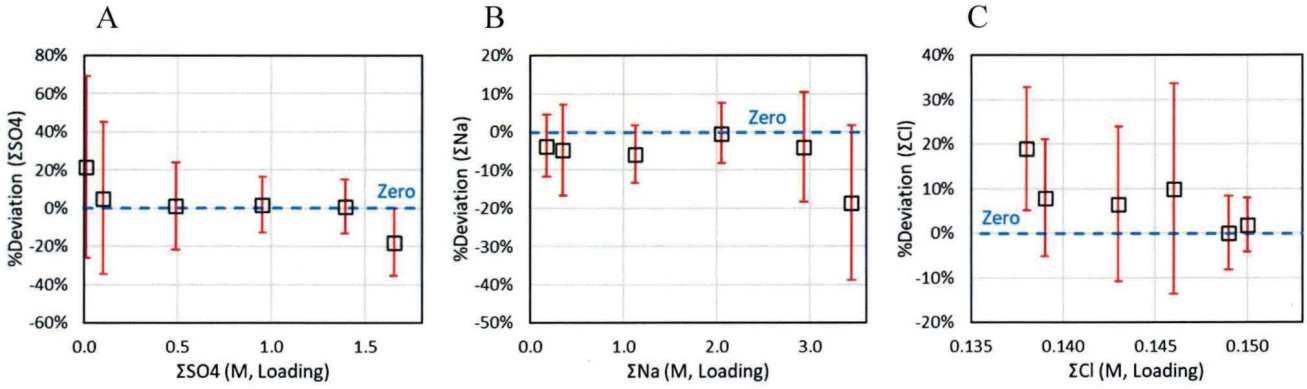
Information Only

Figure VII-1. Plot of ΣPb (Table V-2) vs. ΣSO4 (Table V-3).



The measurements of ΣNa, ΣSO4, and ΣCl are accurate to the loadings within the precision associated with the laboratory operation (Figure VII-2). Exception is the first data point in Figure VII-2C.

Figure VII-2. %Deviations, i.e., Equation (1), of A. ΣSO4, B. ΣNa, C. ΣCl. Error bars are %2SDs.



The uncertainties listed in the Tables of Section V account for the following sources of uncertainty: duplicate reactor preparation per experimental condition, repeated measurements on the duplicates with aging time, sampling methods,[4] use of different bottle materials, human errors associated with filtration, dilution, and instrument operation over long time periods.

No mineralogical transformation of $PbSO_4$(s) (anglesite) was observed (Figure III.1-16 and Figure III.1-17 of GEOC-21-03; Jang et al., 2021).

[4] Repeated sampling from the same reactor vs. Sacrificial sampling from reactor terminated at the prescribed time of investigation.

Information Only

VIII. Model Parameterization: Pitzer Approach

The pHr and Molarity (M, mol/L) of Section V are converted to pmH and molality (m, mol/kg) using the solution properties (Table VIII-1) and Equation (2). M:m is the Molarity-to-molality conversion factor, the unit being L/kg (Jang, 2020). The pmH and molalities are presented in Table VIII-2. The pH correction factor, A, was calculated using Equation (3), which is applicable to Na_2SO_4 dominated solutions (Roselle, 2011). A converts pHr to pcH via Equation (4). pcH and pmH are the negative base 10 logarithms of the concentration of H^+ in Molarity and molality, respectively. pmH is calculated using Equation (5).

$$M \times M{:}m = m \quad (2)$$

$$A = 0.0332 \cdot I^2 - 0.203 \cdot I - 0.016 \quad (3)$$

$$pcH = pHr + A \quad (4)$$

$$pmH = pcH - \log M{:}m \quad (5)$$

where I is the ionic strength in Molarity scale.

Table VIII-1. Properties of Solutions made of Na_2SO_4 and NaCl.

Na_2SO_4, m	NaCl, m	M:m, L/kg	I, M	A (correction factor)
0.01	0.15	1.0027	0.03	-0.02
0.10	0.15	1.0073	0.30	-0.07
0.50	0.15	1.0278	1.46	-0.24
1.0	0.15	1.0535	2.86	-0.32
1.5	0.15	1.0791	4.17	-0.29
1.8	0.15	1.0945	4.95	-0.21

I: ionic strength, M: Molarity, A converts pHr to pcH via Equation (4). pcH is defined right under Section VIII.

Table VIII-2. Molality (m, mol/kg) of the measurements.

pmH		ΣPb, m		ΣSO4, m		ΣNa, m		ΣCl, m	
Average	2SD	Average	2SD	Average	2SD	Average	2SD	Average	2SD
2.74	0.24	6.95E-05	1.16E-05	1.22E-02	5.81E-03	1.64E-01	1.33E-02	1.53E-01	9.26E-03
3.06	0.16	2.74E-05	1.31E-05	1.06E-01	4.21E-02	3.35E-01	4.00E-02	1.50E-01	1.25E-02
3.21	0.14	3.46E-05	8.86E-06	5.07E-01	1.17E-01	1.08E+00	8.27E-02	1.65E-01	3.89E-02
3.17	0.18	5.10E-05	2.03E-05	1.02E+00	1.48E-01	2.15E+00	1.72E-01	1.61E-01	2.79E-02
3.26	0.18	7.06E-05	2.47E-05	1.51E+00	2.14E-01	3.04E+00	4.37E-01	1.62E-01	2.12E-02
3.33	0.23	8.44E-05	1.65E-05	1.48E+00	2.60E-01	3.07E+00	6.22E-01	1.80E-01	2.48E-02

Kolthoff et al. (1942) reported the solubility of $PbSO_4$(s) (anglesite) in solutions of Na_2SO_4 (Excerpt VIII-1, Table VIII-3) and H_2SO_4 (Excerpt VIII-2, Table VIII-4). Uncertainty of the measurements and

Information Only

methods for pH control were not reported therein. While their experiments were conducted in lower and narrower range of ΣSO4 than Table VIII-2 and the equilibration time did not exceed 80 hours, their experiments *did not* contain Cl^-, i.e., simpler system than the experiments in Section IV to observe the Pb^{+2} - SO_4^{-2} chemistry without Cl^- interference. They will be concurrently considered in the model parameterization of this memo. The measurements in Table VIII-2, Table VIII-3, and Table VIII-4 are plotted in Figure VIII-1.

Excerpt VIII-1. Table 1 of Kolthoff et al. (1942). $PbSO_4$(s) - Na_2SO_4 - H_2O.

TABLE 1

Solubility of lead sulfate in sodium sulfate solutions at 25°C. ± 2°

MOLARITY OF Na_2SO_4	SOLUBILITY OF LEAD SULFATE	
	Milligrams of Pb per liter	Moles of $PbSO_4$ per liter × 10^5
0	31.5	15.2
0.001	4.8	2.4
0.01	3.3	1.6
0.02	2.9	1.4
0.04	2.7	1.3
0.08	2.7	1.3
0.100	3.4	1.6
0.200	3.9	1.9
0.350	4.8	2.3
0.500	4.8	2.3

Table VIII-3. Measurements transcribed from Excerpt VIII-1. See text for last two columns.

Na2SO4, M	PbSO4, M	I, M	M:m, L/kg	ΣPb, m	ΣSO4, m	ΣNa, m	Log K_{Davies}	Log K_{PACE}
0	1.52E-04	6.08E-04	0.9991	1.52E-04	1.52E-04	0.00E+00	-7.73	-7.77
0.001	2.32E-05	3.09E-03	0.9992	2.31E-05	1.02E-03	2.00E-03	-7.83	-7.86
0.01	1.59E-05	3.01E-02	0.9996	1.59E-05	1.00E-02	2.00E-02	-7.36	-7.42
0.02	1.40E-05	6.01E-02	1.0001	1.40E-05	2.00E-02	4.00E-02	-7.29	-7.39
0.04	1.30E-05	1.20E-01	1.0011	1.30E-05	4.01E-02	8.01E-02	-7.22	-7.39
0.08	1.30E-05	2.40E-01	1.0032	1.31E-05	8.03E-02	1.61E-01	-7.10	-7.43
0.100	1.64E-05	3.00E-01	1.0042	1.65E-05	1.00E-01	2.01E-01	-6.96	-7.36
0.200	1.88E-05	6.00E-01	1.0093	1.90E-05	2.02E-01	4.04E-01	NA [A]	-7.45
0.350	2.32E-05	1.05E+00	1.0171	2.36E-05	3.56E-01	7.12E-01	NA	-7.55
0.500	2.32E-05	1.50E+00	1.0251	2.37E-05	5.13E-01	1.03E+00	NA	-7.71
						Average:	-7.36	-7.53
						2SD:	0.64	0.36

[A] NA: Not applicable since Davies equation is limited to I < 0.5 M (Stumm and Morgan, 1996).

Information Only

165 Excerpt VIII-2. Table 3 of Kolthoff et al. (1942). $PbSO_4$(s) - H_2SO_4 - H_2O.

TABLE 3

Solubility of lead sulfate in sulfuric acid at 25°C.

MOLARITY OF H_2SO_4	SOLUBILITY OF LEAD SULFATE	
	Milligrams of Pb per liter	Moles of $PbSO_4$ per liter × 10^5
0.001	7.2	3.6
0.005	4.5	2.2
0.0075	4.4	2.2
0.010	3.6	1.8
0.025	3.6	1.8
0.050	3.4	1.7
0.100	3.2	1.6
0.250	3.6	1.8
0.500	4.2	2.1

166

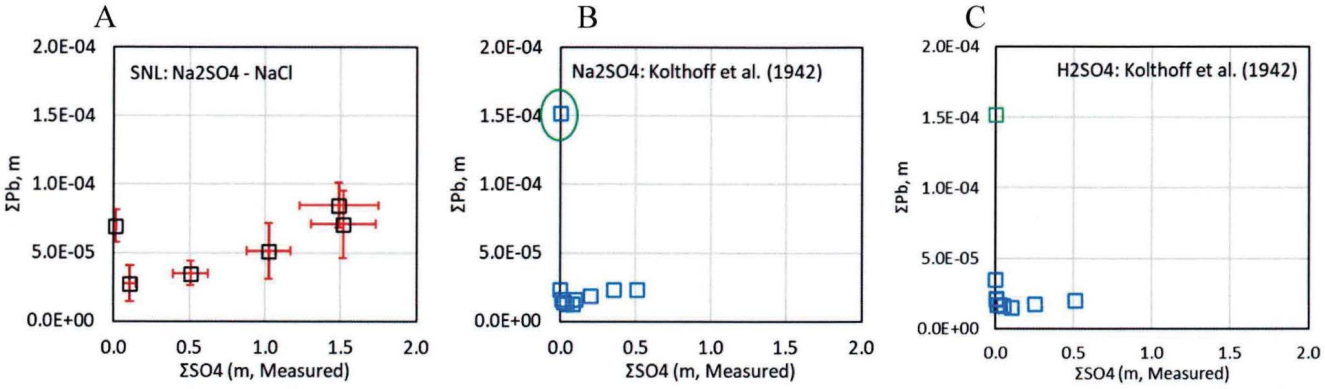
167 Table VIII-4. Measurements transcribed from Excerpt VIII-2. See text for last two
168 columns.

H2SO4, M	PbSO4, M [A]	I, M	M:m, L/kg	ΣPb, m	ΣSO4, m	ΣH, m	Log K_{Davies}	Log K_{PACE}
0.001	3.5E-05	0.003	0.9990	3.5E-05	1.0E-03	2.0E-03	-7.65	-7.66
0.005	2.2E-05	0.015	0.9992	2.2E-05	5.0E-03	1.0E-02	-7.39	-7.38
0.0075	2.1E-05	0.023	0.9993	2.1E-05	7.5E-03	1.5E-02	-7.30	-7.29
0.010	1.7E-05	0.030	0.9994	1.7E-05	1.0E-02	2.0E-02	-7.33	-7.31
0.025	1.7E-05	0.075	0.9999	1.7E-05	2.5E-02	5.0E-02	-7.16	-7.14
0.050	1.6E-05	0.15	1.0008	1.6E-05	5.0E-02	1.0E-01	-7.08	-7.09
0.100	1.5E-05	0.30	1.0026	1.5E-05	1.0E-01	2.0E-01	-6.99	-7.12
0.250	1.7E-05	0.75	1.0079	1.8E-05	2.5E-01	5.0E-01	NA [B]	-7.20
0.500	2.0E-05	1.50	1.0170	2.1E-05	5.1E-01	1.0E+00	NA	-7.36
						Average	-7.27	-7.28
						2SD:	0.44	0.35

169 [A] Calculated from the values in "Milligrams of Pb per liter" column of Excerpt VIII-2 using atomic weight of Pb = 207.2
170 g/mol. It is unclear why the differences are observed between the values in this column and the values in "Moles of $PbSO_4$
171 per liter × 10^5" column of Excerpt VIII-2.
172 [B] NA: Not applicable since Davies equation is limited to I < 0.5 M (Stumm and Morgan, 1996).

Information Only

Figure VIII-1. Plots of measurements in A. Table VIII-2, B. Table VIII-3, C. Table VIII-4. No uncertainty reported for B and C. The green square in C is the same as the square marked with green oval in B. It represents the solubility of $PbSO_4$(s) in water without addition of Na_2SO_4 nor H_2SO_4.



The thermodynamic solubility constant for $PbSO_4$(s), i.e., K of Reaction (6) denoted K(6) hereafter, can be expressed as in Equation (7).

$$PbSO_4(s) = Pb^{+2} + SO_4^{-2} \quad (6)$$

$$K = \{Pb^{+2}\}\cdot\{SO_4^{-2}\} = <Pb^{+2}>\cdot[Pb^{+2}]\cdot<SO_4^{-2}>\cdot[SO_4^{-2}] = <Pb^{+2}>\cdot<SO_4^{-2}>\cdot{}^cK \quad (7)$$

In Equation (7), K is the thermodynamic solubility constant at I = 0; { .. }, < .. >, [..] are the activity, activity coefficient, concentration; ^cK is the conditional solubility constant defined by the concentrations of Pb^{+2} and SO_4^{-2} at a certain ionic strength, i.e.,

$$^cK = [Pb^{+2}]\cdot[SO_4^{-2}] \quad (8)$$

Using the measurements in Table VIII-3 and Table VIII-4, the thermodynamic solubility constant for Reaction (6) can be calculated using selected activity coefficient equations. For example, using the measurements in the first row of Table VIII-3, the conditional solubility constant, i.e., the ^cK in Equation (8), can be determined as in Equation (9);

$$^cK = [Pb^{+2}]\cdot[SO_4^{-2}] = (1.52\times10^{-4})^2 = 2.31\times10^{-8} = 10^{-7.63} \quad (9)$$

The values for $<Pb^{+2}>$ and $<SO_4^{-2}>$ can be calculated using the Davies Activity Coefficient Equation, Equation (10) (Stumm and Morgan, 1996);

$$\text{Log} < i > = -A\cdot z_i^2\cdot\left(\frac{\sqrt{I}}{1+\sqrt{I}} - 0.2\cdot I\right) \quad (10)$$

where A = 0.5, z_i = charge of the species i, $I = 0.5\Sigma z_i^2\cdot[i]$. Davies Activity Coefficient Equation is known to be applicable when I < 0.5 M (Stumm and Morgan, 1996).

Information Only

197 $I = 0.5 \cdot 2 \cdot 4 \cdot (1.52 \times 10^{-4}) = 6.08 \times 10^{-4}$ m, thus, log $<Pb^{+2}>$ = log $<SO_4^{-2}>$ = -0.0478 via Equation (10).
198 Therefore, by Equation (7), the thermodynamic solubility constant consistent with the Davies equation
199 is;

200 $$K_{Davies} = <Pb^{+2}> \cdot <SO_4^{-2}> \cdot {}^{c}K = 10^{(-0.0478 \times 2)} \times 10^{-7.63} = 10^{-7.73} \quad (11)$$

201 The values for $<Pb^{+2}>$ and $<SO_4^{-2}>$ can be calculated with the Pitzer Activity Coefficient Equation
202 (PACE) using the thermodynamic quantities for Na^+, HSO_4^-, SO_4^{-2}, H^+, OH^- in Harvie et al. (1984).
203 When the measurements in the first row of Table VIII-3 were run through EQ3NR (Wolery and Jarek,
204 2003),

205 $$<Pb^{+2}> = 10^{-0.067} \quad (12)$$

206 and

207 $$<SO_4^{-2}> = 10^{-0.065} \quad (13)$$

208 Thus, the thermodynamic solubility constant per PACE is;

209 $$K_{PACE} = <Pb^{+2}> \cdot <SO_4^{-2}> \cdot {}^{c}K = 10^{(-0.067 - 0.065)} \times 10^{-7.63} = 10^{-7.77} \quad (14)$$

210 Likewise, the rest of log K_{Davies} and log K_{PACE} in the last two columns in Table VIII-3 and Table VIII-4
211 were calculated. In both Tables, the log K_{PACE} were confined within narrower 2SD. The log K_{Davies}
212 and log K_{PACE} in Equations (11) and (14) are close to each other, indicating that they are useful
213 approximations to the true log K(6) because the resulting difference between the two activity
214 coefficient models are minimal at $I = 6.08 \times 10^{-4}$ m ≈ 0 m. Giordano (1989) and Wahman et al.
215 (2021) reported -7.81 and -7.79 for log K(6), respectively.

216 Up to this point, no thermodynamic quantities for Pb(II) species has been implemented. First set of
217 thermodynamic quantities to be implemented is the set for Pb^{+2} - Cl^- chemistry (Table VIII-5, Table
218 VIII-6), which are validated for ΣCl up to 6 m and consistent with Harvie et al. (1984) (GEOC-21-11;
219 Jang et al., 2021). The log K values in Table VIII-5 were validated to ΣCl up to 6 m using PIPs in
220 Table VIII-6 in Jang (2021, Revisit ...). Results of the calculation engaging the thermodynamic
221 quantities in Table VIII-5 and Table VIII-6 in addition to Harvie et al. (1984) are presented in Figure
222 VIII-2.

223 Table VIII-5. Reactions and the log Ks for Pb^{+2} - Cl^- system at 25 °C, I = 0 (GEOC-21-
224 11; Jang et al., 2021).

Reaction	LogK	Reference
Aqueous reactions		
$PbCl^+ = Pb^{2+} + Cl^-$	-1.48±0.01	Millero and Byrne (1984), Jang (2021, Revisit) (6 m)

Information Only

$PbCl_2(aq) = Pb^{2+} + 2Cl^-$	-2.03±0.01	Millero and Byrne (1984), Jang (2021, Revisit) (6 m)
$PbCl_3^- = Pb^{2+} + 3Cl^-$	-1.86±0.01	Millero and Byrne (1984), Jang (2021, Revisit) (6 m)
Dissociation reaction		
$PbCl_2(s)$ (cotunnite) $= Pb^{2+} + 2Cl^-$	-4.83	Edwards et al. (1992)

Table VIII-6. PIPs supporting the species in Table VIII-5 above.

i	j	α_1/α_2[A]	$\beta^{(0)}$	$\beta^{(1)}$	$\beta^{(2)}$	C^ϕ	Source
H^+	$PbCl_3^-$	2.0/12.0	0.1077	0.0425	0.00	-0.0035	Jang (2021, Revisit) (6 m)
Na^+	$PbCl_3^-$	2.0/12.0	-0.10025	0.0	0.0	0.0	Section V.3.8 (GEOC-21-11; Jang et al., 2021)
Mg^{+2}	$PbCl_3^-$	2.0/12.0	0.23015	0.0	0.0	0.0	Section V.4.8 (GEOC-21-11; Jang et al., 2021)

Green fonts: not relevant to this memo. Cited for completeness.

[A] α_1 and α_2 are pre-set constants used in the Pitzer activity coefficient equation. α_1 and α_2 apply for only cation-anion binary pair. α_2 is not applied when $\beta^{(2)}$ is zero or not used. Unit for α_1 and α_2 is $kg^{1/2} \cdot mol^{-1/2}$ (Pitzer, 1991).

Figure VIII-2. Application of the log K_{PACE} = -7.77, i.e., Equation (14), in combination with the thermodynamic quantities in Table VIII-5 and Table VIII-6 in addition to Harvie et al. (1984) to the three set of data in Figure VIII-1. A-1, B-1, and C-1 are on the same scale. A-2, B-2, and C-2 are in individual scales to show the details.

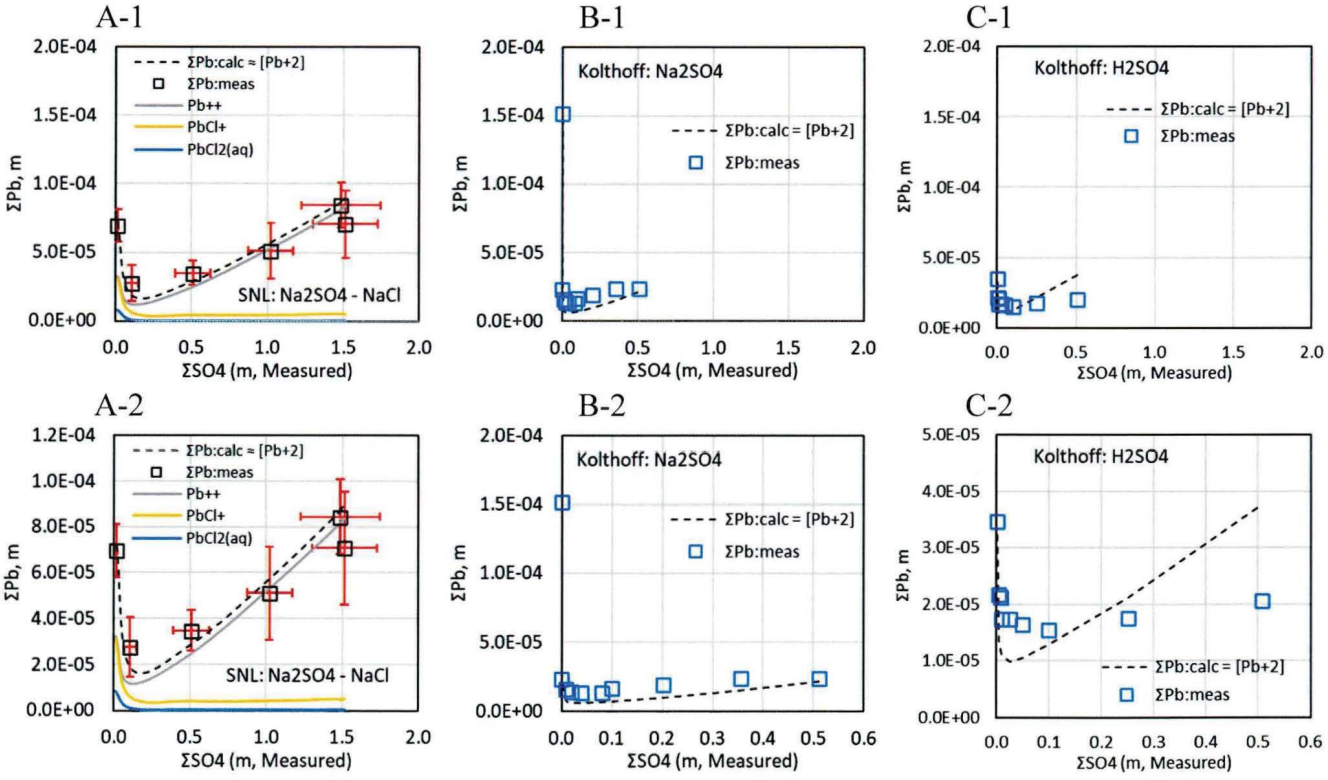


Figure VIII-2A-(1,2) indicates that the data set in Table VIII-2 can be represented by the model within the uncertainty of the measurements using the log Ks and PIPs in Harvie et al. (1984), Table VIII-5, Table VIII-6, in addition to the log K(14) = -7.77. Inclusion of additional log Ks or PIPs in the model

Information Only

would be considered statistically identical to the prediction delineated in Figure VIII-2A-(1,2). Interactions of species pairs, such as Pb^{+2}/HSO_4^- and Pb^{+2}/SO_4^{-2}, were not needed.

Application of the same thermodynamic quantities as above to the measurements of Kolthoff et al. (1942) is displayed in Figure VIII-2B-(1,2) (Na_2SO_4 experiment) and Figure VIII-2C-(1,2) (H_2SO_4 experiment). The Pb^{+2} - Cl^- chemistry (Table VIII-5, Table VIII-6) does not materialize in Figure VIII-2B,C-(1,2) because Cl^- was not used in the two experiments. The uncertainty associated with the measurements of Kolthoff et al. (1942) were not reported therein. PIPs for species pairs like Pb^{+2}/HSO_4^- and Pb^{+2}/SO_4^{-2} are not considered.

Based on the measurements of Kolthoff et al. (1942) (Table VIII-3, Table VIII-4), Paige et al. (1992) determined the log K of $PbSO_4$(s), i.e., log K(6), to be -7.76, as well as the PIPs for the species pairs of Pb^{+2}/HSO_4^- and Pb^{+2}/SO_4^{-2} (Table VIII-7).

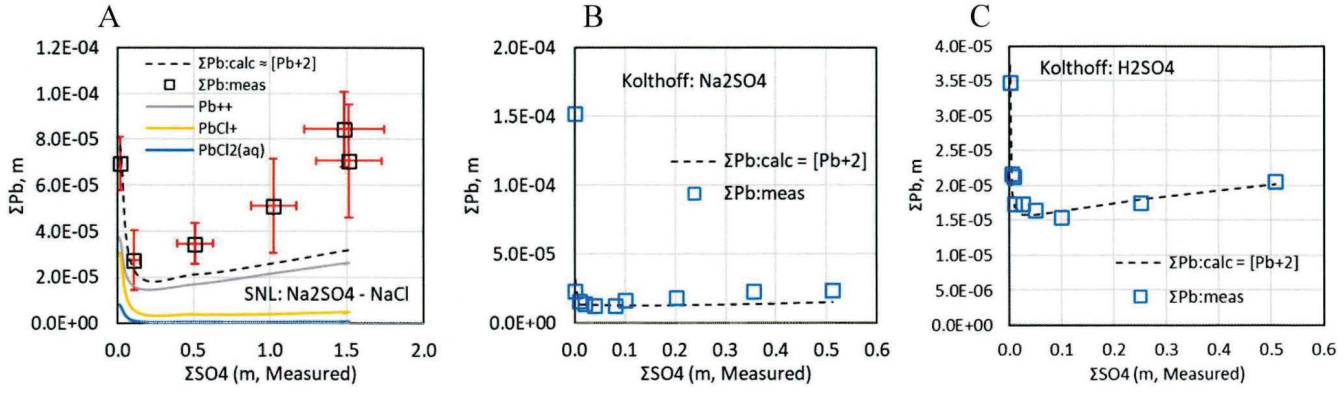
Table VIII-7. PIPs determined in Paige et al. (1992) using the measurements of Kolthoff et al. (1942). LogK(6) = -7.76 in Paige et al. (1992). Not part of conclusion of this memo.

i	j	α_1/α_2[A]	$\beta^{(0)}$	$\beta^{(1)}$	$\beta^{(2)}$	C^{φ}
Pb^{+2}	HSO_4^-	2.0/12.0	0.2719	1.839	0.0	0.0
Pb^{+2}	SO_4^{-2}	1.4/12.0	0.00	4.368	-129	0.0

[A] α_1 and α_2 are pre-set constants used in the Pitzer activity coefficient equation. α_1 and α_2 apply for only cation-anion binary pair. α_2 is not applied when $\beta^{(2)}$ is zero or not used. Unit for α_1 and α_2 is $kg^{1/2} \cdot mol^{-1/2}$ (Pitzer, 1991).

Implementation of the log K(6) = -7.76 and PIPs in Table VIII-7 (Paige et al., 1992) together with those in Harvie et al. (1984), Table VIII-5, and Table VIII-6 are displayed in Figure VIII-3. The log Ks of -7.77 and -7.76 seems of no statistical difference for the first and second data in Figure VIII-2A and Figure VIII-3A. Major differences between Figure VIII-2 and Figure VIII-3 occur due to the use of the PIPs of Paige et al. (1992) (Table VIII-7).

Figure VIII-3. Application of the log K for $PbSO_4$(s) of -7.76 and the relevant PIPs of Paige et al. (1992) to the three sets of measurements in Figure VIII-1. Not part of conclusion of this memo.



Information Only

Implementation of the PIPs of Paige et al. (1992) resulted in a fit outside the uncertainty bounds of the measurements given in Table VIII-2. The fit is presented by the dashed line in Figure VIII-3A. The apparent improvements in Figure VIII-3B and C should be taken for granted, because Paige et al. (1992) used the measurements of Kolthoff et al. (1942) to calibrate their log K(6) = -7.76 and PIPs in Table VIII-7. The improvement of the fit over $0 < \Sigma SO4 < 0.1$ m in Figure VIII-3B was made by fitting $\beta^{(1)}$ and $\beta^{(2)}$ for the species pair Pb^{+2}/SO_4^{-2}. SO_4^{-2} is the major anionic species in the Na_2SO_4 experiment at circumneutral pH by Reaction (15) below. The improvement of the fit in Figure VIII-3C was made by fitting $\beta^{(0)}$ and $\beta^{(1)}$ for the species pair Pb^{+2}/HSO_4^- to decrease $\Sigma Pb \equiv [Pb^{+2}]$ by increasing $<Pb^{+2}>$ at a given $\{Pb^{+2}\}$. HSO_4^- is one of the major anionic species in the H_2SO_4 experiment in the acidic solution by Reaction (15).

$$HSO_4^- = H^+ + SO_4^{-2} \quad (15)$$

where log K(15) = -1.97 (Harvie et al., 1984).

However, Kolthoff et al. (1942) did not evaluate their measurements with uncertainties, therefore, it is unclear how Paige et al. (1992) justified the use of the four fitting parameters ($\beta^{(1)}$ and $\beta^{(2)}$ for Pb^{+2}/SO_4^{-2}; $\beta^{(0)}$ and $\beta^{(1)}$ for Pb^{+2}/HSO_4^-; Table VIII-7). That is, the model predictions in Figure VIII-2B,C-(1,2) and Figure VIII-3B,C could be considered statistically of no difference when the users of the model of Paige et al. (1992) apply arbitrary uncertainties to the measurements of Kolthoff et al. (1942).

The ranges of ΣSO4 investigated by Kolthoff et al. (1942) (up to ~0.5 m) are lower and narrower than the range covered by the measurements in Table VIII-2 (up to ~1.5 m), and the ΣPb are less than 2×10^{-4} m in Kolthoff et al. (1942). It is deemed difficult to expect significant ionic interactions between Pb^{+2} vs. SO_4^{-2} (or HSO_4^-) at such low concentrations of ΣPb and ΣSO4 in Kolthoff et al. (1942).

The underestimation of ΣPb (dashed line in Figure VIII-3A) results from the suppression of $[Pb^{+2}]$ (gray line in Figure VIII-3A). The suppression is caused by the elevation of $<Pb^{+2}>$ using the PIPs in Paige et al. (1992) (Table VIII-7). This observation indicates that the PIPs of Paige et al. (1992) calibrated at lower and within a narrower range of ΣSO4 concentrations with unreported uncertainties could be an overparameterization. Their PIPs make the model underestimate the measurements obtained at higher and within wider range of ΣSO4 (Figure VIII-3A).

Powell et al. (2009) determined the log Ks for $PbSO_4$(aq) and $PbSO_4$(s) (Table VIII-8). Their log Ks were scaled to I = 0 using an SIT activity model. It is recommended to implement the SIT-log Ks in the speciation calculation in combination with the SIT parameters, i.e., ε's. The ε's are the counterpart

Information Only

of PIPs in SIT activity model. As such, after implementing the SIT-log Ks in PACE-based speciation calculation of this memo, the need of PIPs to support the SIT-based logKs will be gauged.

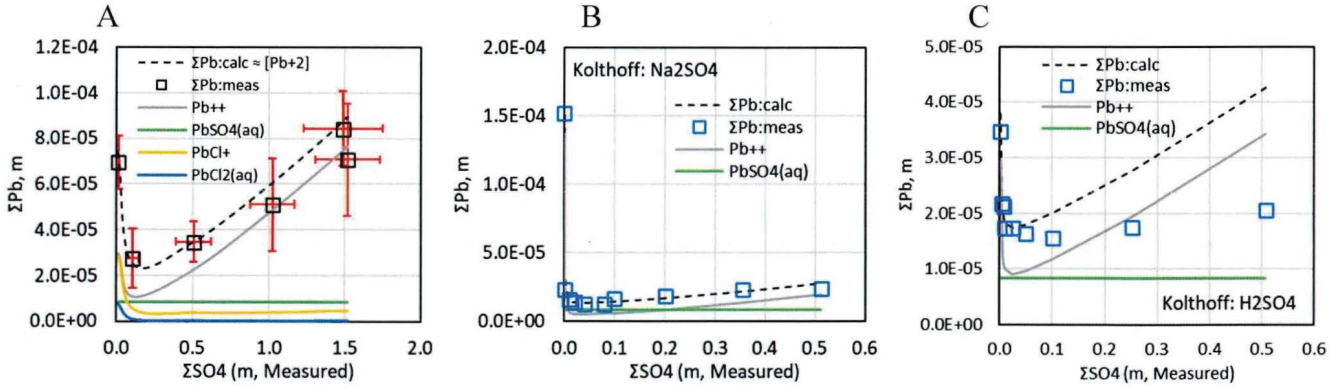
Table VIII-8. Log Ks of $PbSO_4$(s) and $PbSO_4$(aq) suggested in Powell et al. (2009). Not part of conclusion of this memo.

Reaction	Log K	Reference
Aqueous reactions		
$PbSO_4(aq) = Pb^{+2} + SO_4^{-2}$	-2.72 ± 0.05	Powell et al. (2009)
$Pb(SO_4)_2^{-2} = Pb^{+2} + 2SO_4^{-2}$	ND [A]	Table A2-10 of Powell et al. (2009), p.2467
Dissociation reaction		
$PbSO_4$(s) (Anglesite) = $Pb^{+2} + SO_4^{-2}$	-7.80 ± 0.05	Powell et al. (2009)

[A] ND: Not Determined

Results of calculation using the SIT-log Ks in Table VIII-8 (Powell et al., 2009) are displayed in Figure VIII-4. The model behavior in Figure VIII-4 showed similarity with Figure VIII-2, where neither PIPs or the new complex were considered. By allowing the formation of the complex, $PbSO_4$(aq), the ΣPb are elevated (dashed lines in Figure VIII-4 compared with those in Figure VIII-2). The elevation of ΣPb in Figure VIII-4A is statistically of no difference from Figure VIII-2A-(1,2). Again, because no uncertainties were reported in Kolthoff et al. (1942), the statistical significance of the dashed lines in Figure VIII-4B,C cannot be established.

Figure VIII-4. Application of log Ks for $PbSO_4$(aq) and $PbSO_4$(s) of Powell et al. (2009) (Table VIII-8) to the three sets in Figure VIII-1. Not part of conclusion of this memo.



The observations made in Figure VIII-2, Figure VIII-3, and Figure VIII-4 indicate the following: (i) The implementation of new complex, $PbSO_4$(aq), did not result in significant change (compare Figure VIII-2 with Figure VIII-4),[5] and (ii) the activity correction for the species Pb^{+2} by PIPs of Paige et al.

[5] No need to install PIP for $PbSO_4$(aq) as the counterpart of epsilon in SIT because (i) SIT does not account for the neutral - ion interaction, and (ii) statistical differences cannot be concluded.

Information Only

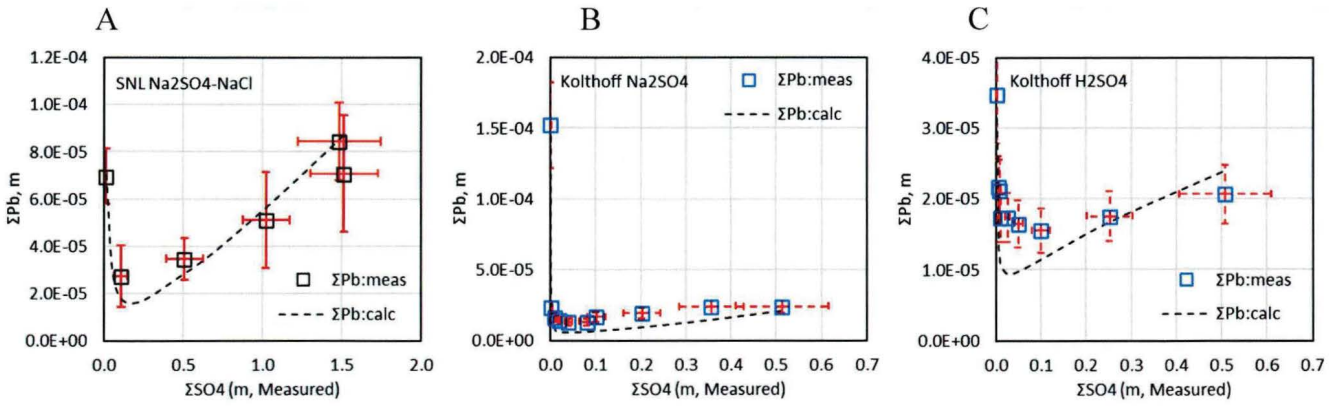
(1992) apparently improved the fit for the measurements of Kolthoff et al. (1942).[6] However, the activity correction by the PIPs of Paige et al. (1992) resulted in a significant suppression of the predicted concentrations for the measurements by SNL WIPP Geochemistry (Table VIII-2) (compare Figure VIII-2 with Figure VIII-3). This indicates a possibility where the activity correction made by Paige et al. (1992) for the H_2SO_4 experiment of Kolthoff et al. (1942) can be an overparameterization based on unreported uncertainties.

The H_2SO_4 solutions used in Kolthoff et al. (1942) contains both SO_4^{-2} and HSO_4^- at concentrations comparable to each other via Reaction (15), therefore, at least one of the two sets of PIPs of Paige et al. (1992), i.e., one for Pb^{+2}/SO_4^{-2}, the other for Pb^{+2}/HSO_4^-, can be subject of refitting.

A few trial fits made for the H_2SO_4 experiments of Kolthoff et al. (1942) indicated that one of the remaining candidates for further fitting is the PIP for the species pair Pb^{+2}/H^+, denoted $\theta(Pb^{+2}/H^+)$ hereafter. Fitting the PIPs for Pb^{+2}/SO_4^{-2} and Pb^{+2}/HSO_4^- placed the model representation of the SNL data set in Table VIII-2 outside the uncertainty bounds. Adjustment of the $\theta(Pb^{+2}/H^+)$ would leave the predictions of the Na_2SO_4 (- NaCl) experiments unaffected due to the lower $[H^+]$ relative to the H_2SO_4 experiment of Kolthoff et al. (1942).

Application of $\theta(Pb^{+2}/H^+) = 0.343$ in combination with the thermodynamic quantities used for Figure VIII-2 is displayed in Figure VIII-5 with an arbitrarily assumed ±20% uncertainty for the experiments of Kolthoff et al. (1942).

Figure VIII-5. Implementation of PIP for Pb^{+2}/H^+, i.e., $\theta(Pb^{+2}/H^+) = 0.343$, in addition to the thermodynamic quantities in Harvie et al. (1984), Table VIII-5, Table VIII-6, and log K(6) = log K_{PACE} = -7.77. Dashed error bars in B and C represent an arbitrarily assumed ±20% uncertainty for the measurements of Kolthoff et al. (1942).



[6] which can be considered for granted due to the fact that the PIPs of Paige et al. (1992) were calibrated using the measurements of Kolthoff et al. (1942).

IX. Summary

No sign of cumulative complexation Pb^{+2} - SO_4^{-2} was observed. No need of quantifying ionic interaction in the species pairs of Pb^{+2}/SO_4^{-2} and Pb^{+2}/HSO_4^- was identified. The common ion effect realized via suppression of ΣPb when ΣSO4 < 0.1 m. The change of ΣPb ≈ $[Pb^{+2}]$ in Figure VIII-5A can be attributed to the rapid change of $<Pb^{+2}>$ determined by the Debye-Huckel term in the PACE without considering the ionic interaction of Pb^{+2} with SO_4^{-2} or HSO_4^-. If left uncorrected, the model behavior of $<Pb^{+2}>$ resulted in an apparent overestimation in the H_2SO_4 experiment (Figure VIII-2C). Such correction was made through the $\theta(Pb^{+2}/H^+)$ in Figure VIII-5C, instead of the PIPs for Pb^{+2}/SO_4^{-2} and Pb^{+2}/HSO_4^-. The result is to minimize the impact of such correction on the predictions depicted in Figure VIII-5A,B where the $[H^+]$ is lower and, therefore, the correction of $<Pb^{+2}>$ through the $\theta(Pb^{+2}/H^+)$ is minimal.

The solubility constant for Reaction (6), i.e., K(6) = K(14) = K_{PACE} = $10^{-7.77}$, and the PIP for a species pair, Pb^{+2}/H^+, i.e., $\theta(Pb^{+2}/H^+)$ = 0.343, are the new additions to data0.fm1. The thermodynamic quantities for Pb^{+2} - Cl^- system (Table VIII-5, Table VIII-6) were implemented through GEOC-21-11 (Jang et al., 2021). Consideration of PIPs for species pairs, e.g., Pb^{+2}/HSO_4^-, Pb^{+2}/SO_4^{-2}, etc., or complexation constant for such as $PbSO_4$(aq) would be re-evaluated when SNL WIPP Geochemistry finds compelling evidences.

The $\theta(Pb^{+2}/H^+)$ parameter was quantifiable in this memo because Pb^{+2} is the dominant dissolved species of Pb(II) and the postulation of $PbSO_4$(aq) per Powell et al. (2009) did not change the predominance of Pb^{+2}. It is recommended to challenge the accuracy of $\theta(Pb^{+2}/H^+)$ = 0.343 using separate experiments in acidic conditions (e.g., HNO_3 solutions) where the complexation of Pb^{+2} would be minimal.

The thermodynamic quantities used and verified in this memo are summarized in Table IX-1 (reactions and logKs) and Table IX-2 (PIPs). They shall be used in combination with the thermodynamic quantities for Na^+, HSO_4^-, SO_4^{-2}, OH^-, Cl^-, H^+ of Harvie et al. (1984) for model consistency.

Table IX-1. Reactions and the log Ks for I = 0 at 25 °C.

Reaction	Log K	Reference
Aqueous reactions		
$PbCl^+ = Pb^{+2} + Cl^-$	-1.48±0.01	Millero and Byrne (1984), Jang (2021, Revisit) (6 m)
$PbCl_2$(aq) = $Pb^{+2} + 2Cl^-$	-2.03±0.01	Millero and Byrne (1984), Jang (2021, Revisit) (6 m)
$PbCl_3^- = Pb^{+2} + 3Cl^-$	-1.86±0.01	Millero and Byrne (1984), Jang (2021, Revisit) (6 m)
Dissociation reactions		
$PbCl_2$(s) (cotunnite) = $Pb^{+2} + 2Cl^-$	-4.83	Edwards et al. (1992), Jang (2021, Revisit)
$PbSO_4$(s) (anglesite) = $Pb^{+2} + SO_4^{-2}$	-7.77	This memo, in agreement with Powell et al. (2009)

Information Only

371 Table IX-2. PIPs to support the log Ks in Table IX-1.

i	j	α_1/α_2^A	$\beta^{(0)}$	$\beta^{(1)}$	$\beta^{(2)}$	C^φ	Source
H^+	$PbCl_3^-$	2.0/12.0	0.1077	0.0425	0.00	-0.0035	Jang (2021, Revisit) (6 m)
Na^+	$PbCl_3^-$	2.0/12.0	-0.10025	0.0	0.0	0.0	Section V.3.8 (GEOC-21-11; Jang et al., 2021)
Mg^{+2}	$PbCl_3^-$	2.0/12.0	0.23015	0.0	0.0	0.0	Section V.4.8 (GEOC-21-11; Jang et al., 2021)
i	j	θ					Source
Pb^{+2}	H^+	0.343					This memo[7]

372 Green font: not relevant to this memo. Cited for completeness.

373 This memo demonstrates the difficulties of adopting literature-retrieved measurements and model
374 parameters as they are, and emphasizes the critical need of experimental validation of the
375 measurements and parameters of the literature using SNL WIPP Geochemistry's own measurements
376 that are (i) traceable to the Scientific Notebooks and (ii) with quantification of experimental
377 uncertainty. Such experimental validation would be critical to determine and remove model
378 overparameterization using solubility data.

379 If SNL WIPP Geochemistry had confined itself to the WIPP-relevant condition where ΣSO4 = 0.2 m
380 during the model development stage, the PIPs of Paige et al. (1992) would have been accepted because
381 the range of ΣSO4 in Paige et al. (1992) (0 to 0.5 m) encompasses the WIPP-relevant ΣSO4 = 0.2 m.
382 This would have been considered a blind selection of literature model parameters without the need for
383 further verification.

384 Assuming the accuracy of the Pb^{+2} - Cl^- model in Table VIII-5 and Table VIII-6, the measurements in
385 Table VIII-2 can be further processed to isolate the contribution of Pb^{+2} - Cl^- complexation.

386 $$\Sigma Pb = [Pb^{+2}] + \Sigma[Pb^{+2} - Cl^-]_i \quad (16)$$

387 Therefore,

388 $$[Pb^{+2}] = \Sigma Pb - \Sigma[Pb - Cl]_i \quad (17)$$

389 where [..] stand for the concentration of the species, thus, $\Sigma[Pb - Cl]_i$ means the sum of the
390 concentrations of the Pb^{+2} - Cl^- complexes in Table VIII-5, i.e., $PbCl^+$, $PbCl_2(aq)$, and $PbCl_3^-$.

391 The $[Pb^{+2}]$ in Equation (17) represents the dissolved Pb^{+2} that would have been measured in the
392 absence of NaCl as ΣPb, and now can be compared directly with the measurements of Kolthoff et al.
393 (1942) in a ΣPb vs. ΣSO4 space in Figure IX-1, where A and B display the same error bars
394 representing the 2SD in Table VIII-2.

[7] Files associated with the derivation of $\theta(Pb^{+2}/H^+)$ are archived at (CVS/CVSLIB/WIPP_EXTERNAL/anglesite).

Information Only

The Pb^{+2} - Cl^- model in Table VIII-5 and Table VIII-6 is also subject to uncertainty, so an uncertainty propagation model in Equation (18) is adopted from Harris (1987):

$$e_{\Sigma Pb}^2 = e_{[Pb^{+2}]}^2 + e_{\Sigma(Pb-Cl)_i}^2 \quad (18)$$

where $e_{\Sigma Pb}$, $e_{[Pb^{+2}]}$, and $e_{\Sigma(Pb-Cl)_i}$ stand for the %2SD of ΣPb, $[Pb^{+2}]$, and sum of Pb^{+2} - Cl^- complexes, respectively.

As an example, 1:1 contribution of $[Pb^{+2}]$ and $\Sigma(Pb\text{-}Cl)_i$ to the uncertainty of ΣPb is assumed, i.e., Equation (19), and the calculated 2SD for the $[Pb^{+2}]$ are displayed as the orange error bars in Figure IX-1C.

$$e_{[Pb^{+2}]}^2 = e_{\Sigma(Pb-Cl)_i}^2 \quad (19)$$

Therefore,

$$e_{[Pb^{+2}]} = \frac{e_{\Sigma Pb}}{\sqrt{2}} \quad (20)$$

The 1:1 contribution is an assumption to equally weight $e_{[Pb^{+2}]}$ and $e_{\Sigma(Pb-Cl)_i}$ in Equations (18) and (19). Thus, under different ways of weighting the terms using various statistical models in the literature, the length of the orange error bars may vary.

Figure IX-1. Comparison of $[Pb^{+2}]$ calculated from the measurements in Table VIII-2 (black squares) with ΣPb = $[Pb^{+2}]$ in Kolthoff et al. (1942) (blue squares and ×; Table VIII-3, Table VIII-4). Orange error bars in C are the 2SD reduced from the 2SD in Table VIII-2 via Equations (16) to (20). See the text for the reduced 2SD using an uncertainty propagation model in Harris (1987). To display the details, x-axis is in log scale. A. Full scale. B and C. Zoom-in of the area marked with green rectangle in A.

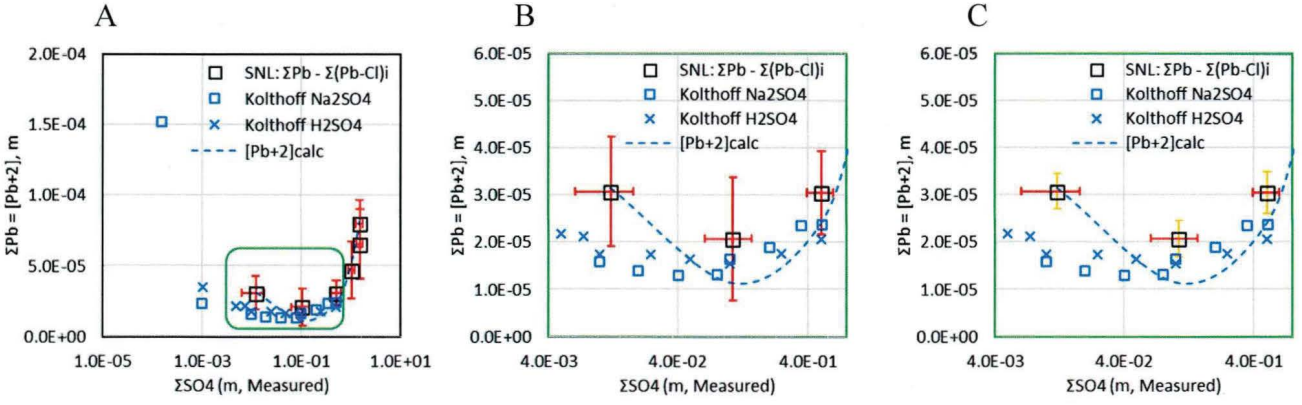


Figure IX-1 indicates that, depending on the uncertainty associated with the measurements of Kolthoff et al. (1942), (i) the measurements in Table VIII-2 can be considered inclusive of the measurements of

Information Only

Kolthoff et al. (1942) when the $\Sigma(Pb\text{-}Cl)_i$ are isolated, (ii) the model prediction (blue dashed line in Figure IX-1B,C) can be considered acceptable for the measurements in Table VIII-2, Table VIII-3, and Table VIII-4, and therefore, (iii) SNL WIPP Geochemistry can state that it reproduced the measurements of Kolthoff et al. (1942).

Boundary between the stability of $PbSO_4(s)$ (anglesite) and $PbCl_2(s)$ (cotunnite) can be located by Reaction (21);

$$PbSO_4(s) + 2Cl^- = PbCl_2(s) + SO_4^{-2} \quad (21)$$

where log K(21) = -2.94.[8] Therefore, the boundary can be expressed by Equation (22);

$$\text{Log } \{SO_4^{-2}\} = 2 \times \text{Log } \{Cl^-\} - 2.94 \quad (22)$$

where { .. } denote the activity of the species inside. The boundary is displayed in blue line in Figure IX-2.

The activity of SO_4^{-2} and Cl^- in a simulated brine (sim-brine) of NaCl = 5.0 m, $MgCl_2$ = 1.0 m, and Na_2SO_4 = 0.2 m can be calculated using the thermodynamic quantities in Harvie et al. (1984);

$$\text{Log } \{SO_4^{-2}\}_{\text{sim-brine}} = -2.30 \quad (23)$$

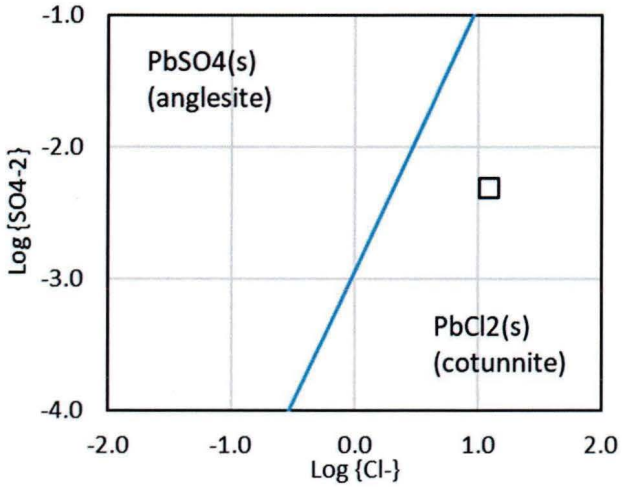
$$\text{Log } \{Cl^-\}_{\text{sim-brine}} = 1.08 \quad (24)$$

which are the coordinate of the square in Figure IX-2, representing the chemical condition of the simulated brine in a log $\{SO_4^{-2}\}$ vs. log $\{Cl^-\}$ space. In the simulated brine, $PbCl_2(s)$ (cotunnite) is the stable solid, which means $PbSO_4(s)$ (anglesite) should not form from a thermodynamic point of view. The simulated brine can be considered WIPP-relevant. Therefore, except for the scientific curiosity (including kinetics), there is no need to further investigate the Pb^{+2} - SO_4^{-2} system for the thermodynamic model synthesis effort of SNL WIPP Geochemistry. The log K of $PbSO_4(s)$ in Table IX-1 will be added to the SNL WIPP Geochemical Thermodynamic Database for completeness, expecting the database to be applicable for other applications, e.g., hydrometallurgy, ore processing, etc. They will be included in the CRA-related calculations.

[8] -2.94 = Log K($PbSO_4(s)$) - Log K($PbCl_2(s)$) = -7.77 - (-4.83) (Table IX-1).

Information Only

Figure IX-2. Stability fields of $PbSO_4$(s) (anglesite) and $PbCl_2$(s) (cotunnite). Rectangle represents the chemical condition of a simulated brine made of NaCl = 5.0 m, $MgCl_2$ = 1.0 m, and Na_2SO_4 = 0.2 m. In the simulated brine, $PbCl_2$(s) is the stable solid.



X. ACKNOWLEDGMENT

Technical review was performed by Carlos Jove-Colon. QA review was performed by Catrina Carrillo and Shelly Nielsen. Management review was performed by Chammi Miller. Comments and resolutions were archived under SNL WIPP QA Program. The author thanks the reviewers for constructive comments.

XI. REFERENCES

XI.1. A

Arnold, R., and J. Jang, 2022. Results of Temperature Monitoring in Three Gloveboxes in SNL WIPP NPHB. Memo to SNL WIPP Records Center, 1/6/2022. Sandia National Laboratories, Carlsbad, New Mexico, U.S.A. ERMS 576538.

XI.2. E

Edwards, R., R. D. Gillard, P. A. Williams, and A. M. Pollard, 1992. Studies of secondary minerals formation in the PbO - H_2O - HCl system. Mineralogical Magazine, 56, 53-65.

XI.3. G

Giordano, T. H., 1989. Anglesite ($PbSO_4$) solubility in acetate solutions: The determination of stability constants for lead acetate complexes to 85 °C. Geochimica et Cosmochimica Acta, 53, 359-366.

XI.4. H

Harris, D. C., 1987. Quantitative Chemical Analysis. W. H. Freeman and Company, New York.

Information Only

Harvie, C. E., N. Møller, and J. H. Weare, 1984. The prediction of mineral solubilities in natural waters: The Na-K-Mg-Ca-H-Cl-SO_4-OH-HCO_3-CO_3-CO_2-H_2O system to high ionic strengths at 25°C. Geochimica et Cosmochimica Acta, 48, 723-751.

XI.5. J

Jang, J., 2020. Factors for Conversion of Molarity to molality and molality to Molarity. Memo to SNL WIPP Records Center and SNL WIPP Geochemistry. October 16, 2020. Sandia National Laboratories, Carlsbad, New Mexico, U.S.A. ERMS 574276.

Jang, J., 2021. Revisit to the Pitzer Geochemical Thermodynamic Model for the $PbCl_2$(s) - HCl - H_2O System. Memo to SNL WIPP Records Center and SNL WIPP Geochemistry, May 25, 2021. Sandia National Laboratories, Carlsbad, New Mexico, U.S.A. ERMS 575309.

Jang, J., P. Hora, L. Kirkes, C. Miller, and L. Zhang, 2021. Analysis Report documenting the Assessment of the Solubility of Lead, EDTA and other Organic Ligands in non-Sulfide systems performed under TP 08-02 and under TP 20-01. Revision 0. GEOC-21-03. Sandia National Laboratories, Carlsbad, New Mexico, U.S.A. ERMS 576387.

Jang, J., P. Hora, L. Kirkes, C. Miller, and L. Zhang, 2021. Analysis Report documenting Solubility and Complexation of Iron, Lead, Magnesium, Neodymium, and Boron in the WIPP-Relevant Brines under TPs 06-03, 08-02, 12-02, 14-03, 14-05, 16-02, 19-01, and 20-01. Revision 0. GEOC-21-11. Sandia National Laboratories, Carlsbad, New Mexico, U.S.A. ERMS 576381.

XI.6. K

Kolthoff, I. M., R. W. Perlich, and D. Weiblen, 1942. The Solubility of Lead Sulfate and of Lead Oxalate in Various Media. J. Phys. Chem., 46, 561-570.

XI.7. M

Millero, F. J. and Byrne, R. H., 1984. Use of Pitzer's equations to determine the media effect on the formation of lead chloro complexes. *Geochimica et Cosmochimica Acta* 48, 1145-1150.

XI.8. P

Paige, C. R., W. A. Kornicker, O. E. Hileman Jr., and W. J. Snodgrass, 1992. Modelling solution equilibria for uranium ore processing: The $PbSO_4$-H_2SO_4-H_2O and $PbSO_4$-Na_2SO_4-H_2O systems. Geochimica et Cosmochimica Acta, 56(3), 1165-1173.

Pitzer, K. S., 1991. Ion interaction approach: Theory and data correlation. In: Pitzer, K. S. (Ed.), *Activity Coefficients in Electrolyte Solutions, 2nd Edition.* CRC Press, Boca Raton, Florida.

Powell, K. J., P. L. Brown, R. H. Byrne, T. Gajda, G. Hefter, A.-K. Leuz, S. Sjoberg, and H. Wanner. 2009. Chemical speciation of environmentally significant metals with inorganic ligands. Part 3: The Pb^{2+} + OH^-, Cl^-, CO_3^{2-}, SO_4^{2-}, and PO_4^{3-} systems (IUPAC Technical Report), Pure Appl. Chem., Vol. 81, No. 12, 2425-2476.

Information Only

XI.9. R

Roselle, G. T., 2011. Determination of pC_{H+} Correction Factors in Brines. Sandia National Laboratories, Carlsbad, New Mexico, U.S.A. ERMS 556699.

XI.10. S

Stumm, W., and J. J. Morgan, 1996. *Aquatic Chemistry*. John Wiley & Sons, New York.

XI.11. W

Wahman, D. G., M. D. Pinelli, M. R. Schock, and D. A. Lytle, 2021. Theoretical equilibrium lead(II) solubility revisited: Open source code and practical relationships. AWWA Water Science, 3(5), e1250.

Wolery, T., and R. L. Jarek, 2003. Software User's Manual, EQ3/6, Version 8.0,[9] 01/01/2003. ERMS 548926.

(No broken link found by Jay Jang on 01/30/2023. Total line number = 514 including this line)[10]

[9] Also applicable to EQ3/6, Version 8.0a.

[10] If the underlined number does not match with the line number in the left margin, please let J. Jang know to fix the links embedded in this document.

WIPP:4.4.2.2.1:PA:QA-L:558083
Information Only